Chemistry SELECT

www.chemistryselect.org

A journal of ChemPubSoc Europe

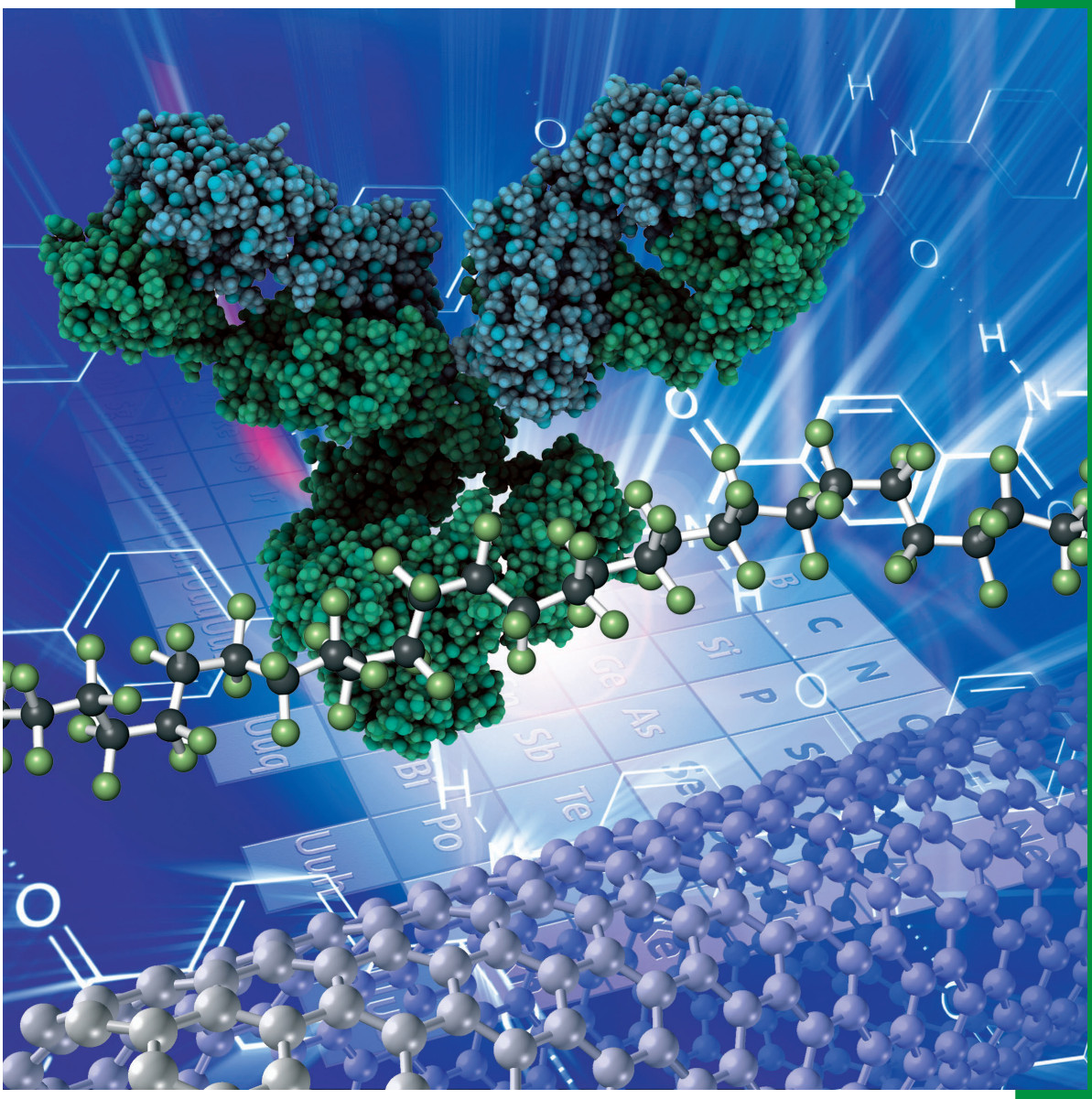

REPRINT

WILEY-VCH

Materials Science inc. Nanomaterials & Polymers

Selective Reduction Sites on Commercial Graphite Foil for Building Multimetallic Nano-Assemblies for Energy Conversion

Rakesh K. Pandey[+],[a, b, c] Satoshi Teraji[+],[a] Siowling Soh,*[b] and Hideyuki Nakanishi*[a]

Selective reduction sites are important for systematically building alloy nanostructure assemblies on various substrates. Utilizing a galvanic exchange protocol, in the present study, multimetallic alloy-type nanostructures were developed on selective reduction sites, which were found to exist on the edges of a commercial graphite foil. Notably, the evaluated method is environmentally friendly and involves sustainable techniques. It was determined that a ternary alloy nanostructure on graphite, consisting of Au, Pd, and Ni, exhibits superior catalytic activity toward ethanol electro-oxidation reaction in an alkaline medium in comparison to the corresponding unimetallic or bimetallic alloy nanostructures. Correspondingly, a bimetallic Fe and Ni-based alloy material on graphite was shown to display improved oxygen evolution reaction response.

Introduction

Graphite foil exhibits a characteristic layered structure consisting of stacked graphene layers separated by a fixed van der Waals distance.[1,2] High surface area and high electrical conductivity make graphite a remarkably useful electrode material for various electrochemical energy applications. Commercial graphite foil displays a defect rich structure containing numerous step edges on the surface, which expose the inner layers.[1,3] Graphite and other similar carbon materials, such as graphene and single walled carbon nanotubes (SWNTs), have been previously reported to function as mild reducing agents able to reduce noble metal salts, including Au, Pt, and Pd.[4–5] Notably, we recently found that owing to the chemical properties of the step edges of commercial graphite foil, it is thermodynamically feasible to also reduce various non-noble metals salts, such as those of Fe and Ni, under ambient conditions.[6] It was observed that the reduction process primarily occurs at step edges, which are separated by the boundaries of the individual graphite microcrystallites and modified with hydroxyl moieties. Since numerous step edges and defects are present on a commercially available graphite foil, high reactivity toward reduction of these metal ions is typically observed. Based on the previous discoveries, in the present study, we demonstrate the possibility of utilizing the selective reduction sites on graphite foil to build multimetallic nanostructure assemblies. In recent years, the galvanic exchange method, which uses the Kirkendall's effect to yield multimetallic assemblies, has attracted significant attention.[7] The approach relies on the principle that a metal with a lower positive standard electrode potential acts a sacrificial template for another metal exhibiting a more positive electrode potential, giving rise to a core-shell type of multimetallic structures. Accordingly, in our method, when a metal salt with a less positive standard electrode potential, or in other words, a metal salt of a less noble metal, such as Ni, is reduced on graphite foil, the product occupies nearly all of the available reduction sites (Graphite/Ni). Thus, when another metal salt exhibiting higher positive standard electrode potential, such as Pd, is subsequently reduced on this Graphite/Ni surface, it is essentially reduced on the previously deposited metal domains (e.g., Ni), resulting in the formation of Graphite/PdNi. This is a consequence of the unavailability of the graphite reduction sites. Analogously, another more noble metal, such as Au, can be further deposited on the bimetallic nanostructure-modified graphite surface to yield Graphite/AuPdNi. Thus, by employing this method, which avoids random deposition of individual metal nanostructures, the selective growth of ternary nanostructures on a commercial graphite foil surface is achievable. The entire process of the formation of the multimetallic nanostructures is schematically illustrated in Figure 1. In addition, the entire process is environmentally friendly, sustainable, requires minimal use of hazardous chemicals, and does not involve any complex equipment.

Several studies on bimetallic alloy catalyst materials for various electrochemical reactions have been reported in the field of electrocatalysis.[7–12] In particular, Pd and Au-based

[a] Dr. R. K. Pandey,[+] S. Teraji,[+] Prof. H. Nakanishi
Department of Macromolecular Science and Engineering, Graduate School of Science and Technology, Kyoto Institute of Technology, Matsugasaki, Kyoto 606-8585, Japan
E-mail: hnakanis@kit.ac.jp
[b] Dr. R. K. Pandey,[+] Prof. S. Soh
Department of Chemical and Biomolecular Engineering, National University of Singapore, 4 Engineering Drive 4, Singapore 117585, Singapore
E-mail: chessl@nus.edu.sg
[c] Dr. R. K. Pandey[+]
Current Address: Department of Chemistry, Mahatma Gandhi Central University, Motihari (East-Champaran), Bihar 845401, India
[+] These authors contributed equally to this work.

Supporting information for this article is available on the WWW under https://doi.org/10.1002/slct.202003185

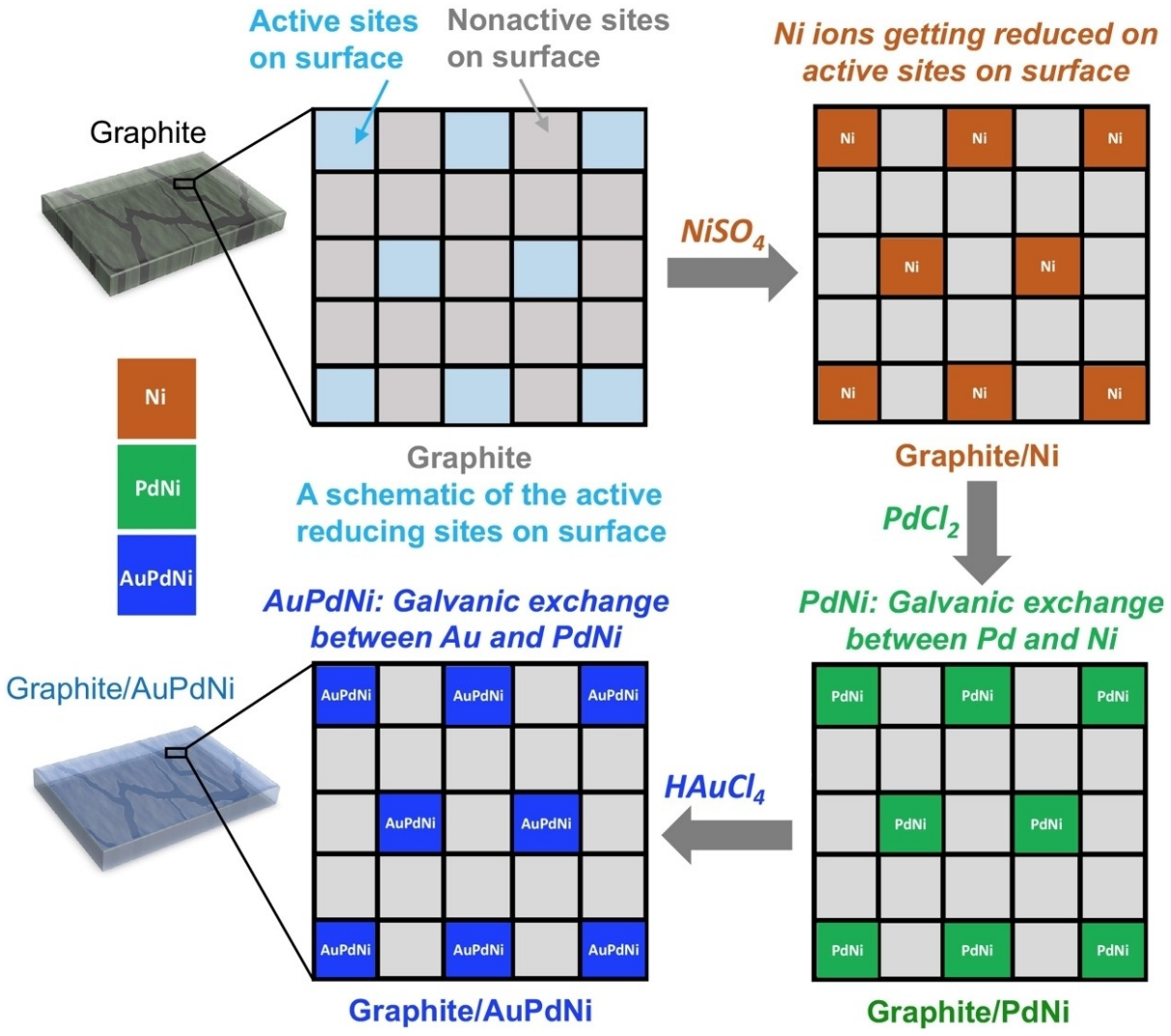

Figure 1. A schematic representation of the multimetallic catalyst formation on graphite utilizing a simple method involving immersion in the metal salt.

bimetallic nanostructures have been investigated for the electro-oxidation of small organic molecules. Notably, it was observed that the catalytic response could be tuned by varying the composition of each metal in the alloy.[10,13–14] The superior catalytic activity of Pd-Au-type alloys is due to the ability of Au, which prevents species (e.g., CO) that poison the EOR reaction from being adsorbed on Pd. Moreover, the electronic coupling effect resulting from the modification of the electronic structure of the catalyst (i.e., Pd) through d-state hybridization may also a key factor.[11] Furthermore, recent studies concerning Pd and Ni-based bimetallic nanostructures for the electro-oxidation reactions of methanol,[15] formic acid,[16] and ethanol[17] have also been reported. It was found that incorporating oxophilic metals, such as Ni, Ru, and Ag in Pd nanostructures enhanced the production of of hydroxyl (OH) radicals, resulting in high catalytic activity.[9,15–16,18] Nevertheless, an increased number of active sites and the distance between the active sites on multimetallic catalysts play a crucial role in the process.

In the present study, the multimetallic nanostructures deposited by selective reduction on graphite were determined to show enhanced catalytic activity in the ethanol electro-oxidation reaction (EOR). In particular, a ternary alloy nanostructure consisting of Au, Pd, and Ni was found to be a remarkable catalytic material exhibiting better performance than the previously studied Au and Pd bimetallic alloys. In addition, we also observed an improved oxygen evolution reaction (OER) response of the bimetallic Fe and Ni-based alloy material fabricated on graphite.

Results and Discussion

The development of the multimetallic structure consisting of Au, Pd, and Ni on graphite was achieved according to the following steps. In the first instance, a 1 cm × 1 cm piece of commercial graphite foil was immersed in the solution of $NiSO_4$ (0.1 M). The Ni salt was selected based on the most negative standard electrode potential of the considered metals (Au, Pd,

and Ni), i.e., Ni is the least noble metal of the three.[19–20] We carried out the experiment by immersing the graphite piece into the $NiSO_4$ salt solution for different lengths of time to obtain a Graphite/Ni electrode. As shown in our previous work, Ni ions are reduced on the step edges of graphite, forming Ni (0) assemblies (Graphite/Ni). Subsequently, Ni(0) undergoes further oxidation in air and ultimately forms a core-shell type Ni/Ni oxide structure.[6]

The obtained Graphite/Ni material was then evaluated as a working electrode using a 3-electrode electrochemical cell containing 0.1 M NaOH as the electrolyte, a large area Pt as the counter electrode, and Ag/AgCl as the reference electrode. Ni and NiO-based electrodes are known to undergo the following redox reaction under alkaline conditions:[21]

$$Ni(OH)_2 + OH^- \leftrightharpoons NiOOH + e^- + H_2O$$

We determined that the charge of the above electrochemical conversion (calculated from the area of the reduction wave) is not dependent on the Ni deposition time on the graphite foil and a rather variable response was observed (Figure S1). This indicates the presence of a varying number of reaction sites on the surface of each graphite sample.

It is noteworthy that at a fixed deposition time, the charge systematically rises with the increase in the Ni salt concentration (Figure 2a,b), suggesting that the deposition of Ni on graphite depends on the concentration of the Ni salt. The Graphite/Ni electrode was subsequently washed using deionized water and kept in the solution of $PdCl_2$ (0.1 M) for approx. 5 min to yield Graphite/PdNi. We optimized the immersion time to 5 min based on the effective response of the resulting catalyst. The Pd ions exhibit a more positive standard electrode potential than the Ni ions; therefore, Pd can replace Ni in an oxidation process, converting Ni metal to Ni ions and resulting in the formation of bimetallic PdNi nanostructures on graphite. The conducted cyclic voltammetry (CV) analysis of Graphite/PdNi demonstrated a clear Pd oxide reduction region, in addition to the Ni response (Figure 2b). Similarly, upon

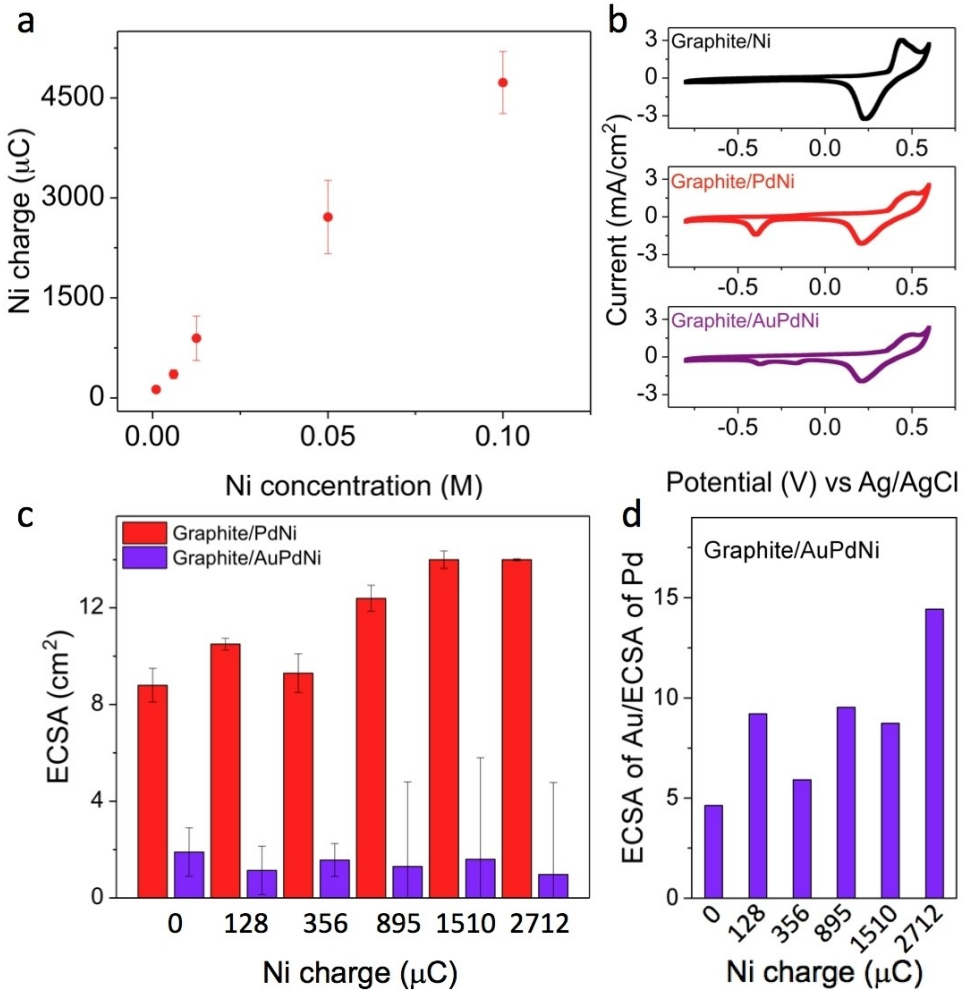

Figure 2. (a) Graphite piece immersed in the $NiSO_4$ salt solution (Graphite/Ni) and charge measured from the reduction wave as a function of the Ni salt concentration. (b) From top to bottom: cyclic voltammetry (CV) analyses of Graphite/Ni, Graphite/PdNi, and Graphite/AuPdNi in 0.1 M NaOH solution (scan rate: 50 mV/s). (c) A comparison of the electrochemically active surface area (ECSA) of Pd measured for Graphite/PdNi and Graphite/AuPdNi. (d) Ratio of the ECSA of Au to that of Pd for Graphite/AuPdNi sample.

immersion of this piece of Graphite/PdNi in $HAuCl_4 \cdot 4H_2O$ (0.02 M) for approx. 30 s, a Graphite/AuPdNi electrode is produced. The CV of Graphite/AuPdNi shows the oxide reduction peak for the Au oxides, along with previous features corresponding to the Pd and Ni species (Figure 2b). The cyclic voltammogram reveals that the catalytic elements, Au, Pd, and Ni, are all exposed on the surface of the nanostructures of the ternary alloy. Based on the high reactivity of the Au salt, we optimized the conditions, which involved lowering the concentration and decreasing the deposition time in comparison to those utilized for the Pd salt. A higher concentration or a longer deposition time would result in complete removal of the Ni and Pd species from the graphite surface, leading to the formation of Graphite/Au as the sole product.[7]

Furthermore, the electrochemically active surface area (ECSA) of Pd in Graphite/PdNi was measured from the charge under the oxide stripping peak using CV analysis in 0.5 M NaOH at 100 mV/s (Figure 2c). Intriguingly, we observed that the increase in the Ni charge on graphite directly correlates with the Pd deposition on graphite, which is believed to have occurred on the already deposited Ni species. This observation can be rationally explained by the extensive presence of Ni in the active sites of the graphite surface. Consequently, the Pd ions could not be effectively reduced on bare graphite; however, they were reduced on the Ni surface (on graphite) *via* a galvanic exchange pathway. In Graphite/PdNi, the majority of the active sites were occupied by Ni and Pd; thus, Au replaced Pd, and Ni on the graphite surface to obtain a ternary alloy nanostructure, i.e., AuPdNi, on graphite (Graphite/AuPdNi). ECSA of Pd in Graphite/AuPdNi is demonstrated in Figure 2c and it is also compared to ECSA of Pd in Graphite/PdNi. A large decrease in Pd ECSA in the case of Graphite/AuPdNi suggests the dissolution of the metal by Au (Figure S2). The proportions of the catalytic elements are tunable with the Ni charge (Figure 2d). Moreover, Figure 3 illustrates the scanning electron microscopy (SEM) images obtained for all investigated samples. It can be seen that the bare graphite surface contains numerous defects, which also constitute the reactive sites for the reduction of metal ions. The SEM image of the Graphite/Ni sample shows the presence of small metal nanoparticles (MNPs) of <100 nm on the surface. Additionally, in the magnified image, a thin film of Ni on the graphite surface is also observed. Since Ni is expected to cover the reactive sites on the surface, numerous Ni features on the surface of Graphite/Ni can be noted. On the other hand, the SEM image of Graphite/PdNi shows the presence of relatively large clusters, ranging from 50 nm to a few μm. Lastly, Graphite/AuPdNi exhibits smaller size MNPs (approx. 100 nm). The presence of small size MNPs is a consequence of the galvanic exchange process, which etches out a significant amount of Pd from the surface, resulting in the formation of smaller size multimetallic MNPs. In the magnified image, the rough surface of the multimetallic MNPs can be observed.

This type of structure could be beneficial for electrochemical applications, as it allows ions to easily reach the inner active metal surface (Pd). To get more insight into the structure of the multimetallic MNPs, we carried out elemental mapping using energy dispersive X-ray spectroscopy (EDS) analysis, as shown in Figure 4. Elemental mapping demonstrates that Ni and Pd make up the inner part of the material (Figure 4b,c), while the jagged outside surface is composed largely of the Au domains (Figure 4d). Although due to the sensitivity of this elemental mapping technique, we could not obtain a visible evidence of Ni in Graphite/AuPdNi, a Ni 2p peak in the X-ray photoelectron spectroscopy (XPS) spectra (Figure S3, SI) as well as the reduction peak in Figure 2b were clearly observed (bottom plot). XPS and electrochemical techniques are more sensitive; therefore, we confirmed the existence of Ni on the surface. The overall structure is noteworthy, as Au does not cover the entire surface of PdNi and numerous Pd and Ni domains are exposed (Figure 4e,f). This integrated nanostructure consisting of exposed Pd regions in close vicinity to the Au and Ni regions could be the key to an improved catalytic response. To measure the elemental composition of the Graphite/AuPdNi sample, we employed inductively coupled plasma-optical emission spectrometry (ICP-OES, Spectroblue, Spectro) analysis. The mass ratio Au/Pd/Ni of 6/66/28 wt% was recorded for the sample. A high Pd content in the sample is vital for the enhancement of the catalytic response.

In the field of electro-oxidation of small organic molecules, the growing interest considering multimetallic MNPs is based on multiple factors.[22–23] Firstly, the ensemble effect is noteworthy,[24] wherein a specific assembly of two metals gives rise to new mechanistic functionalities. For example, several metal surfaces have an inherent property of adsorbing a large amount of –OH groups. These adsorbed OH moieties can greatly inhibit the adsorption of poisonous species, such as CO, which considerably improves the overall catalytic response of the catalyst. Secondly, the electronic coupling effect is also significant and involves a charge transfer between metals, resulting in the modification of the electronic structure of the main catalyst metal.[11,15,17,25–26] Finally, the alteration in the lattice strain in the presence of a diverse variety of metals is crucial too, as different spatial arrangement of surface atoms is also known to significantly affect the catalytic performance.[27]

To determine the electrocatalytic response of Graphite/AuPdNi and to compare it with that of simultaneously prepared Graphite/AuPd, Graphite/PdNi, Graphite/Pd, and Graphite/Ni electrodes, we decided to analyze the ethanol EOR in an alkaline medium (1.0 M ethanol, 0.5 M NaOH). Figure 5 shows the EOR responses for the different electrodes. Graphite/Ni (Figure 5a) exhibits an increased current compared to that of the blank electrolyte solution. However, this oxidation current originates at very high positive potentials and therefore it would not be useful for any practical applications. Notably, Graphite/AuPdNi displays the highest peak current, followed by Graphite/AuPd, Graphite/PdNi, and Graphite/Pd, respectively (Figure 5). The obtained currents are higher than those of the piece of graphite with deposited thiol-protected Pd nanoparticles[6] and other materials described in previous studies, such as Pd nanostructures supported on a conducting polymer.[28–29]

The reasons for the superior performance of Graphite/AuPdNi include the synergistic effects of this ternary system,

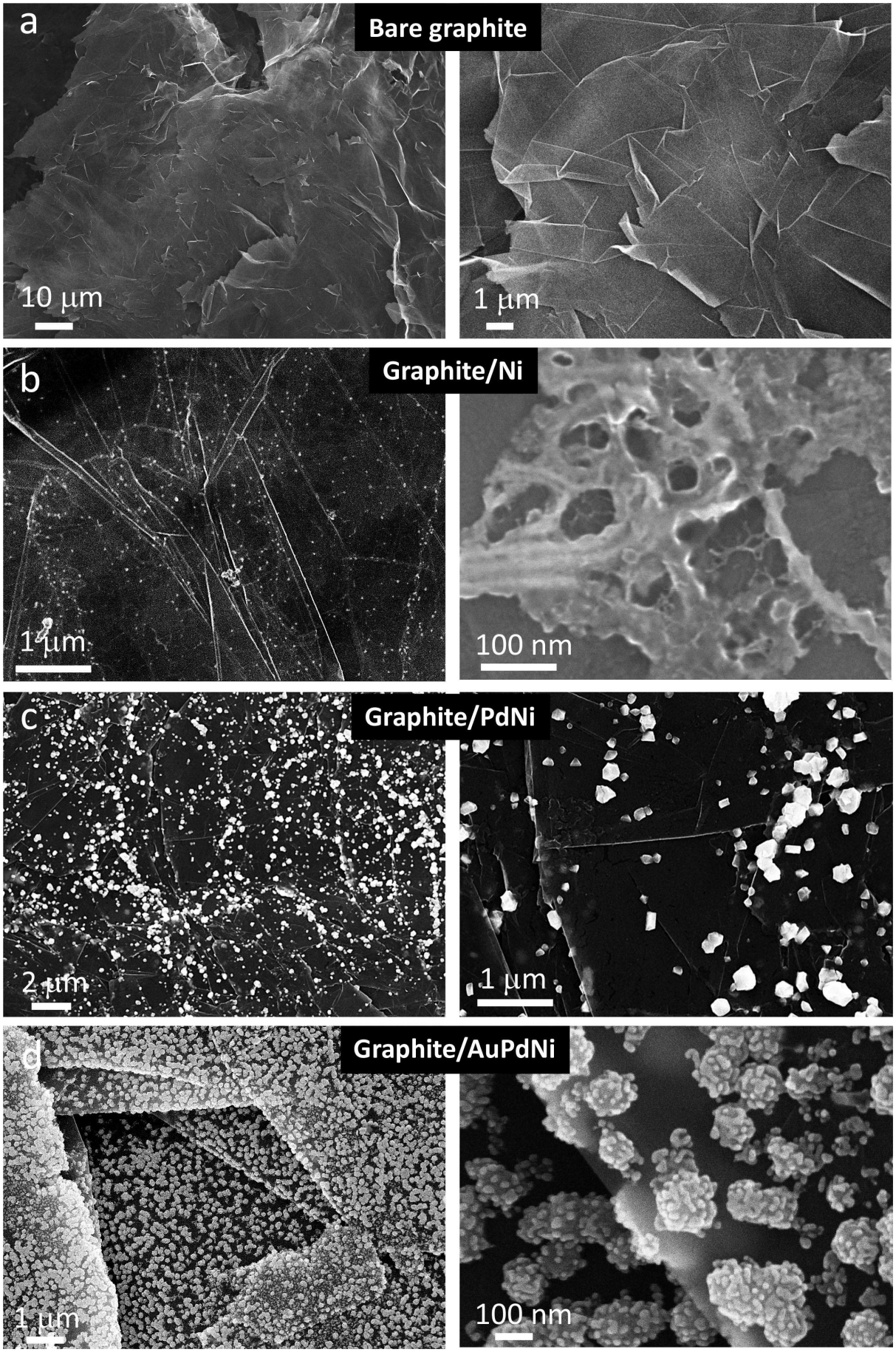

Figure 3. (a) SEM images of (a) bare graphite, (b) Graphite/Ni, (c) Graphite/PdNi and (d) Graphite/AuPdNi. For each sample, the corresponding magnified images are shown on the right.

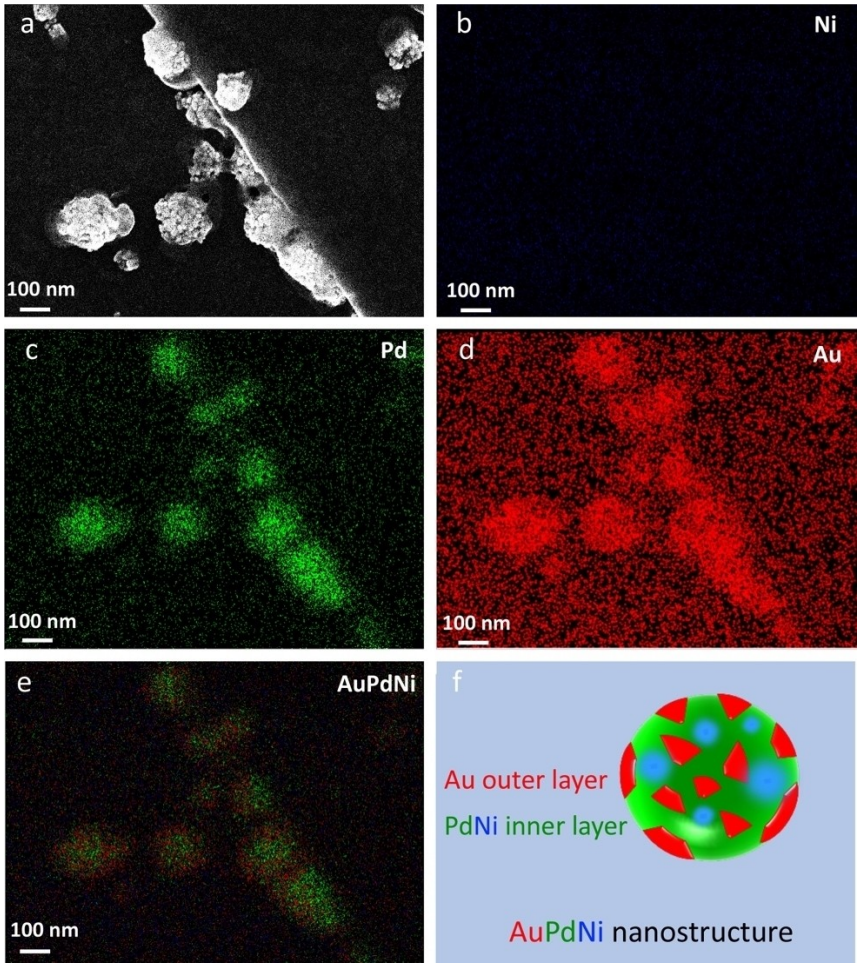

Figure 4. (a) EDS elemental mapping analyses of the multimetallic MNPs on graphite. (a) SEM image of MNPs. Elemental mapping image of (b) Ni, (c) Pd, and (d) Au. (e) A superimposed Au, Pd, and Ni image showing a layer of Au covering the PdNi nanostructures. (f) A schematic representation of the AuPdNi nanostructure composition.

where Au and Ni provide the sites for the adsorption of hydroxide moieties, which in turn allows Pd to exhibit its catalytic activity without being affected by poisonous intermediates, such as CO. A similar mechanism also takes place in the case of Graphite/AuPd; however, for this material, the response is lower than for Graphite/AuPdNi. A probable reason for this could be the fact that in Graphite/AuPdNi, Pd is surrounded by Ni on one side and Au on the other, while in Graphite/AuPd, Pd is surrounded by Au on one side and graphite on the other side. A jagged structure of AuPdNi, shown in Figure 3d also allows an easy access of reactants molecules to reach to the more active surface e.g., Pd. When Pd is surrounded by oxophilic metals, such as Ni on one side, and Au on the other, a greater amount of hydroxide is adsorbed, which results in improved catalytic performance. Moreover, this improved response could also be a consequence of an enhanced electronic coupling effect resulting from the modification of the electronic structure of the main catalyst (i.e., Pd) through d-state hybridization.[10,11] The average peak currents for the Graphite/AuPdNi samples are demonstrated in Figure 5f as a function of the initial Ni reduction peak charge in the respective Graphite/Ni samples.

To further probe the synergistic effect, we also prepared another Graphite/Ni electrode by immersing graphite in a solution of relatively lower Ni concentration (0.02 M $NiSO_4$) to allow some active sites on the substrate to remain empty, as shown in Figure 1a. Subsequently, graphite was immersed in a 0.02 M Au salt to obtain Graphite/AuNi, which was then immersed in a 0.1 M Pd salt solution to yield a Graphite/Pd-AuNi electrode. In this nanostructure assembly, the Pd ions cannot replace Au; therefore, they will reduce and deposit on the remaining selective reduction sites on graphite, creating distinct domains of AuNi and Pd on the graphite surface. This electrode was then subjected to EOR, which exhibited a significantly lower current, mostly attributed to Graphite/Pd (Figure 6a). The outcomes of this experiment suggest that a systematically produced ternary alloy structure (AuPdNi) is required to achieve a better optimized catalytic response, while the distinct domains of metallic nanostructures on graphite are not sufficiently catalytic. The comparison of the peak current densities for all samples is shown in Figure 6b. It can be seen

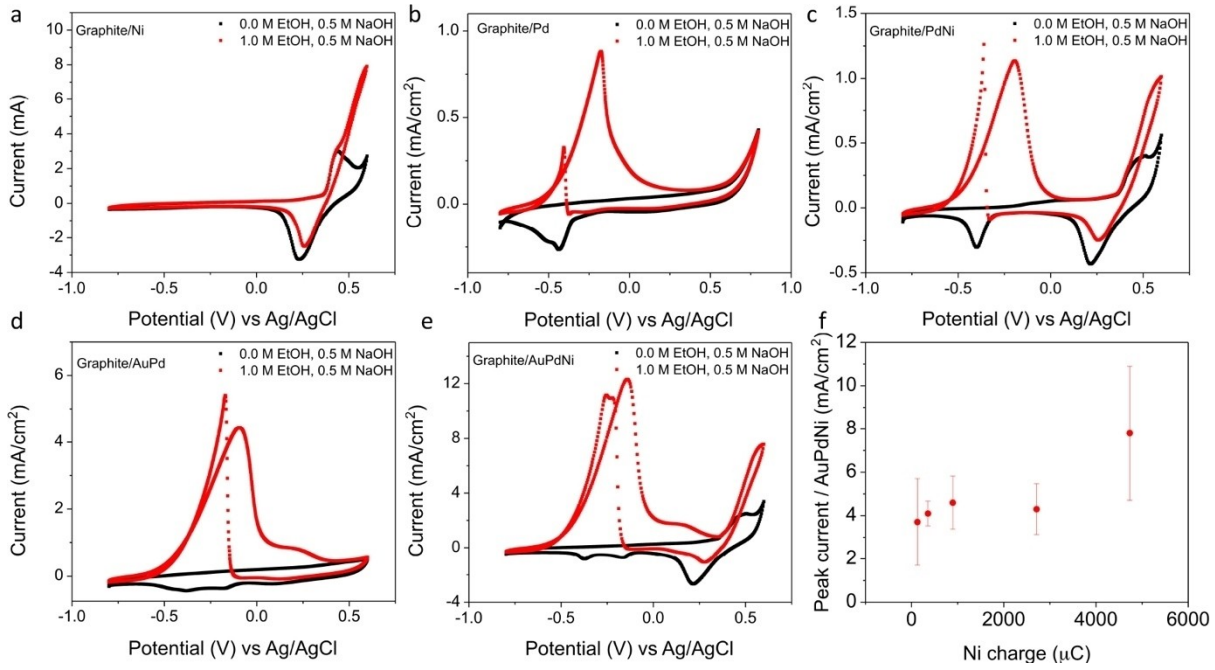

Figure 5. (a) EOR responses (red) of (a) Graphite/Ni, (b) Graphite/Pd, (c) Graphite/PdNi, (d) Graphite/AuPd, and Graphite/AuPdNi in 0.5 M NaOH and 1.0 M EtOH solution. Blank CV in 0.5 M NaOH is also shown for comparison (black). (f) Peak current densities of the Graphite/AuPdNi sample as a function of initial Ni reduction charge in Graphite/Ni.

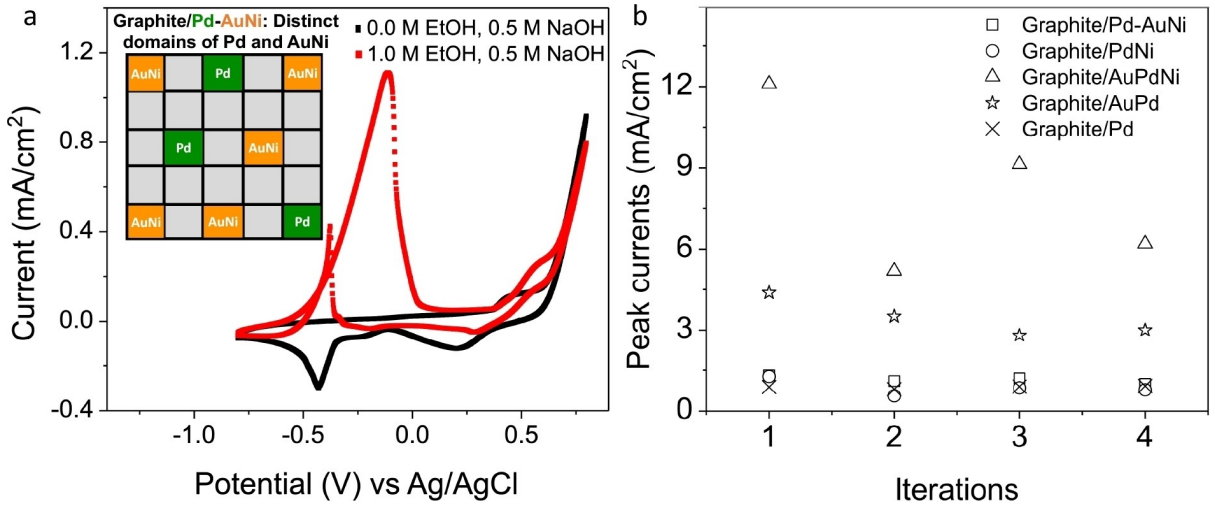

Figure 6. (a) CV curve for EOR at Graphite/Pd-AuNi in 1.0 M EtOH and 0.5 M NaOH. A blank CV curve measured in 0.5 M NaOH is also shown. The inset shows Graphite/Pd-AuNi, comprising of distinct AuNi, and Pd domains on the surface. (b) A comparison of peak current densities for EOR at different electrodes.

that Graphite/AuPdNi consistently exhibited a higher current in comparison to other materials. The catalytic response of the Graphite/AuPdNi was much higher than that recorded in a previous study on Pd metal-based electrode.[30] The catalytic efficiency of the Graphite/AuPdNi sample was also found to be higher than that of the commercial Pd/C sample (Figure S4, SI). We have also made a comparison of the EOR activity of different Pd based electrocatalysts and presented this information in the form of a Table 1, SI.

We have previously demonstrated that the deposition of MNPs also takes place in the bulk of graphite;[6] therefore, it is possible to obtain several flexible catalytic electrodes for various electrochemical energy applications (e.g., flexible fuel cells or supercapacitors) by peeling Graphite/AuPdNi using an adhesive tape.[12,31–32] Thus, the electrodes were obtained by peeling a piece of Graphite/AuPdNi layer by layer using an adhesive tape (inset of Figure 7a). We showed that a peeled piece of Graphite/AuPdNi could be employed as a flexible electrocatalyst electrode for ethanol electro-oxidation (Fig-

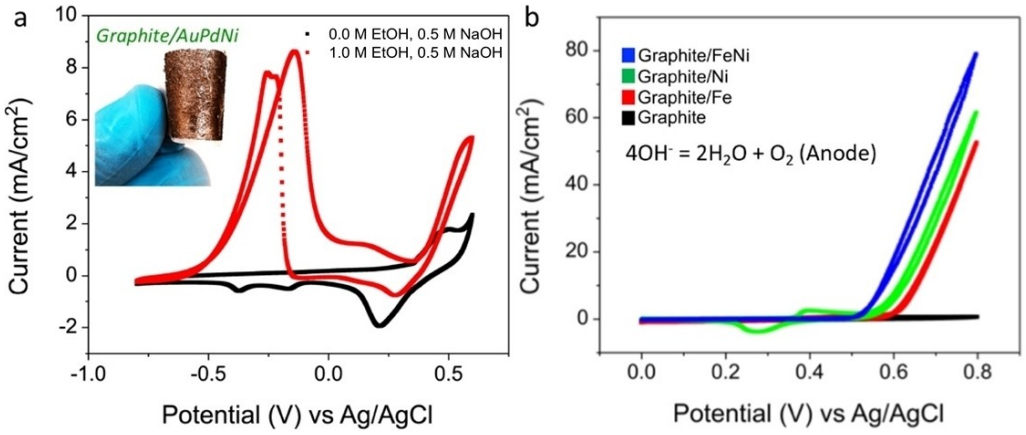

Figure 7. (a) Photograph of a flexible Graphite/AuPdNi electrocatalytic electrode (inset) and its corresponding CV response toward the EOR in 1.0 M ethanol and 0.5 M NaOH. (b) Comparison of OER response of Graphite/FeNi, Graphite/Ni, Graphite/Fe, and graphite (0.5 M NaOH, scan rate: 50 mV/s).

ure 7a). Notably, we observed that the catalytic efficiency of this electrode remained very significant. Moreover, for a 0.5 mm thick piece of Graphite/AuPdNi, several tens of such flexible peeled pieces of graphite/metal can be conveniently obtained.

To further demonstrate the catalytic ability of the multimetallic structure, we prepared a piece of graphite, which contained an alloy of Fe and Ni (Graphite/FeNi). This was achieved by initially immersing the graphite piece for 4 h in 0.1 M $FeSO_4$, and then in 0.1 M $NiSO_4$. We subsequently performed CV measurements in an alkaline medium and found that the materials displayed remarkable catalytic activities for OER (Figure 7b), which were comparable to some previously reported OER catalysts.[33–34] We also noticed that the performance of the OER reaction, utilizing Graphite/FeNi was improved in comparison to the reactions employing Graphite/Ni or Graphite/Fe controls.[6] Specifically, Graphite/FeNi exhibits a lower onset potential and a higher current than Graphite/Ni and Graphite/Fe. We have also made a comparison of the OER activity of different Ni and NiFe based electrocatalysts and presented this information in the form of a Table 2, SI.

Conclusion

In conclusion, it is critical that the methods employed for the fabrication of alternative energy devices are sustainable and environmentally friendly. Such approaches should also be cost-effective and technically simple to allow fast large-scale production. The method involving the synthesis and deposition of multimetallic nanostructures on graphite described in the current study fulfills these requirements. We demonstrated a remarkably simple and environmentally sustainable method, which consists of immersing graphite foil in metal salt solutions to efficiently obtain multimetallic nanostructures on graphite (Graphite/metal). It was determined that graphite acted as a natural template to build multimetallic nanostructure assemblies. The approach was further optimized to construct an Au, Pd, and Ni alloy nanoparticle assembly on graphite (Graphite/AuPdNi). The resulting ternary alloy nanostructure was found to be an effective electrocatalyst material for EOR. Pleasingly, we also noted an efficient OER response of the prepared Graphite/FeNi material. The approach reported in the present study may find valuable applications in constructing effective and economical catalysts for energy conversion.

Supporting Information Summary

Supporting information includes the experimental section and figures and tables with additional information.

Acknowledgments

This work was financially supported by the Ministry of Education, Singapore, under grant R-279-000-408-112 and R-279-000-496-114 (to S.S.), JSPS KAKENHI Grant Numbers JP18H01828 and JP16 K13627 (to H.N.), and the Project for Enhancing Research and Education in Polymer and Fiber Science at KIT (to S.S. & H.N.)
.

Conflict of Interest

The authors declare no conflict of interest.

Keywords: Electrocatalysis · Graphite · Graphene · Galvanic exchange · Nanostructure

[1] A. W. Moore, *Chemistry and physics of carbon*, Marcel Dekker, New York, **1973**, Vol. 11.
[2] R. L. McCreery, *Chem. Rev.* **2008**, *108*, 2646–2687.
[3] C. E. Banks, T. J. Davies, G. G. Wildgoose, R. G. Compton, *Chem. Commun.* **2004**, 829–841.
[4] H. C. Choi, M. Shim, S. Bangsaruntip, H. Dai, *J. Am. Chem. Soc.* **2002**, *124*, 9058–9059.
[5] X. Chen, G. Wu, J. Chen, X. Chen, Z. Xie, X. Wang, *J. Am. Chem. Soc.* **2011**, *133*, 3693–3695.
[6] R. K. Pandey, L. Chen, S. Teraji, H. Nakanishi, S. Soh, *ACS Appl. Mater. Interfaces* **2019**, *11*, 36525–36534.
[7] B. D. Anderson, J. B. Tracy, *Nanoscale* **2014**, *6*, 12195–12216.

[8] X. Teng, Q. Wang, P. Liu, W. Han, A. I. Frenkel, W. Wen, N. Marinkovic, J. C. Hanson, J. A. Rodriguez, *J. Am. Chem. Soc.* **2007**, *130*, 1093–1101.
[9] H. Gao, F. Xiao, C. B. Ching, H. Duan, *ACS Appl. Mater. Interfaces* **2011**, *3*, 3049–3057.
[10] L. Shi, A. Wang, T. Zhang, B. Zhang, D. Su, H. Li, Y. Song, *J. Phys. Chem. C* **2013**, *117*, 12526–12536.
[11] M. Chen, D. Kumar, C. W. Yi, D. W. Goodman, *Science* **2005**, *310*, 291–293.
[12] J. Wang, P. Zhang, Y. Xiahou, D. Wang, H. Xia, H. Mohwald, *ACS Appl. Mater. Interfaces* **2018**, *10*, 602–613.
[13] P. Fang, S. Duan, X. Lin, J. R. Anema, J. F. Li, O. Buriez, Y. Ding, F. Fan, D. Wu, B. Ren, Z. L. Wang, C. Amatore, Z. Tian, *Chem. Sci.* **2011**, *2*, 531–539.
[14] Y. W. Lee, D. Kim, J. W. Hong, S. W. Kang, S. B. Lee, S. W. Han, *Small* **2013**, *9*, 660–665.
[15] M. Zhao, K. Abe, S. Yamaura, Y. Yamamoto, N. Asao, *Chem. Mater.* **2013**, *26*, 1056–1061.
[16] C. Du, M. Chen, W. Wang, G. Yin, *ACS Appl. Mater. Interfaces* **2011**, *3*, 105–109.
[17] L. Chen, L. Lu, Y. Chen, Y. Huang, Y. Li, L. Wang, *Nat. Commun.* **2016**, *8*, 14136–14144.
[18] X. Huang, Z. Zhao, L. Cao, Y. Chen, E. Zhu, Z. Lin, M. Li, A. Yan, A. Zettl, Y. M. Wang, X. Duan, T. Mueller, Y. Huang, *Science* **2015**, *648*, 1230–1234.
[19] A. J. Bard, L. R. Faulkner, *Electrochemical methods: Fundamentals and applications.* Wiley: **2000**.
[20] A. J. Bard, R. Parsons, J. Jordan, *Standard potentials in aqueous solution.* Marcel Dekker: New York, **1985**.
[21] T. Brousse, D. Belanger, J. W. Long, *J. Electrochem. Soc.* **2015**, *162*, A5185-A5189.
[22] K. D. Gilroy, A. Ruditskiy, H. C. Peng, D. Qin, Y. Xia, *Chem. Rev.* **2016**, *116*, 10414–10472.
[23] P. Strasser, S. Koh, T. Anniiyev, J. Greeley, K. More, C. Yu, Z. Liz, S. Kaya, D. Nordlund, H. Ogasawara, M. F. Toney, A. Nilsson, *Nat. Chem.* **2010**, *2*, 454–460.
[24] F. Maroun, F. Ozanam, O. M. Magnussen, R. J. Behm, *Science* **2001**, *293*, 1811–1814.
[25] J. W. Hong, Y. Kim, D. H. Wi, S. Lee, S. Lee, Y. W. Lee, S. Choi, S. W. Han, *Angew. Chem. Int. Ed.* **2016**, *55*, 2753–2758; *Angew. Chem.* **2016**, *128*, 2803–2808.
[26] K. Tedsree, T. Li, S. Jones, C. W. A. Chen, K. M. K. Yu, P. A. J. Bagot, E. A. Marquis, G. D. W. Smith, S. C. E. Tsang, *Nat. Nanotechnol.* **2011**, *6*, 302–307.
[27] P. Moseley, W. A. Curtin, *Nano Lett.* **2015**, *15*, 4089–4095.
[28] R. K. Pandey, V. Lakshminarayanan, *Catal. Lett.* **2014**, *144*, 965–970.
[29] R. K. Pandey, V. Lakshminarayanan, *J. Phys. Chem. C* **2009**, *113*, 21596–21603.
[30] R. K. Pandey, V. Lakshminarayanan, *J. Phys. Chem. C* **2010**, *114*, 8507–8514.
[31] F. Ning, X. He, Y. Shen, H. Jin, Q. Li, D. Li, S. Li, Y. Zhan, Y. Du, J. Jiang, H. Yang, X. Zhou, *ACS Nano* **2017**, *11*, 5982–5991.
[32] Y. Ma, M. Wang, N. Kim, J. Suhr, H. Chae, *J. Mater. Chem. A* **2015**, *3*, 21875–21881.
[33] H. Wang, H. W. Lee, Y. Deng, Z. Lu, P. C. Hsu, Y. Liu, D. Lin, D. Cui, *Nat. Commun.* **2015**, *6*, 7261.
[34] Y. Cheng, S. P. Jiang, *Prog. Nat. Sci.* **2015**, *25*, 545–553.

Submitted: August 12, 2020
Accepted: October 26, 2020